

Kondo impurity between superconducting and metallic reservoir: the flow equation approach

M. Zapalska and T. Domański

Institute of Physics, M. Curie Skłodowska University, 20-031 Lublin, Poland

(Dated: February 7, 2014)

It is well established that a correlated quantum impurity embedded in a metallic host can form the many-body Kondo state with itinerant electrons due to the effective antiferromagnetic coupling. Such effect is manifested spectroscopically by a narrow Abrikosov-Suhl peak appearing at the Fermi level below a characteristic temperature T_K . Recent experiments using nanoscopic heterojunctions where the correlated quantum impurities (dots) are coupled to superconducting reservoirs revealed that the Kondo-type correlations are substantially weaker because: i) the single-particle states of superconductors are depleted around the Fermi level and ii) the on-dot pairing (proximity effect) competes with the spin ordering. Within the Anderson impurity scenario we study here influence of such induced on-dot pairing on the exchange interaction adopting the continuous unitary transformation, which goes beyond the perturbative framework. Our analytical and numerical results show strong detrimental influence of the electron pairing on the effective antiferromagnetic coupling thereby suppressing the Kondo temperature in agreement with the experimental observations.

Motivation – The recent electron tunneling experiments on the self-assembled quantum dots [1], semiconducting nanowires [2, 3] and/or carbon nanotubes [4, 5] coupled to one superconducting and another conducting electrode provided evidence for the subgap bound states. They originate solely from the electron pairing which is spread onto nanoscopic objects activating the anomalous (Andreev) transport channel efficient even when the bias voltage V is smaller than the energy gap Δ of superconductor. Similar in-gap states have been also detected [6–8] in the quantum dots connected to both superconducting reservoirs leading to inversion of the *dc* Josephson current ($0 - \pi$ transition) [9].

Correlated quantum dot (QD) coupled to the external conducting bath does usually induce the effective spin-exchange interactions, which (at low temperatures) may cause its total or partial screening. The resulting Kondo state shows up by a narrow Abrikosov-Suhl peak formed at the Fermi energy. For metallic junctions such effect has been predicted theoretically and observed experimentally [10], enhancing the zero-bias conductance. In the metal - QD - superconductor (N-QD-S) heterostructures the Kondo-type correlations are additionally confronted with electron pairing. Depending on the gate voltage, temperature and potential of the Coulomb repulsion the QD ground state can vary from the (spinful) doublet $|\sigma\rangle$ (where $\sigma = \uparrow, \downarrow$) to the (spinless) BCS configuration $u|0\rangle - v|\uparrow\downarrow\rangle$ [11]. Such quantum phase transitions (showing qualitative influence of the induced on-dot pairing) can be experimentally observed in a tunable way [12].

Interplay between the superconductivity and Kondo-type correlations has been intensively explored experimentally [1–5] and theoretically [13–16]. From a physical point of view the most intriguing situation occurs, when the Kondo and proximity effects eventually coexist, leading to a tiny (yet clearly pronounced) enhancement of the zero-bias subgap conductance reported independently by several groups [1, 3, 17, 18]. Similar zero-bias feature is currently studied also for junctions made of *s*-wave su-

perconductor coupled to quantum wires with the strong spin-orbit interactions (for instance InSb or InAs) where the Majorana-type quasiparticles can appear [19].

In this paper we analyze the proximity induced pairing and study its influence on the antiferromagnetic exchange coupling (thereby on the Kondo temperature) using novel method based on the continuous unitary transformation (CUT). This technique is reminiscent of the renormalization group treatments and has a virtue to go beyond the perturbative scheme. Our study generalizes the famous Schrieffer-Wolf transformation [20] by: i) considering the superconducting bath of itinerant electrons and ii) constructing the non-perturbative procedure reliable for the difficult case when the Kondo-type correlations compete with the induced on-dot pairing. This issue could be presently of a broad interest for the nanoscopic, solid state and ultracold fermion atom communities.

In the following we: 1) introduce the microscopic model of the proximized quantum impurity, 2) construct the continuous canonical transformation expressing it through a set of the *flow* equations, 3) investigate the analytical (lowest order) solution, and 4) discuss the numerical results based on the selfconsistent Runge-Kutta algorithm. Our results reproduce the qualitative features obtained by the subgap tunneling spectroscopy [1–5].

Proximity induced pairing – For studying a combined effect of the electron pairing and the Coulomb repulsion (which can induce the Kondo effect) we consider the Anderson impurity Hamiltonian $\hat{H} = \sum_{\beta} \hat{H}_{\beta} + \sum_{\sigma} \varepsilon_d \hat{d}_{\sigma}^{\dagger} \hat{d}_{\sigma} + U_d \hat{n}_{d\uparrow} \hat{n}_{d\downarrow} + \sum_{\mathbf{k}, \sigma, \beta} \left(V_{\mathbf{k}\beta} \hat{d}_{\sigma}^{\dagger} \hat{c}_{\mathbf{k}\sigma\beta} + V_{\mathbf{k}\beta}^{*} \hat{c}_{\mathbf{k}\sigma\beta}^{\dagger} \hat{d}_{\sigma} \right)$. It formally describes the correlated quantum dot placed in between the normal metal ($\beta = N$) and the superconducting ($\beta = S$) electrodes. As usually, \hat{d}_{σ} ($\hat{d}_{\sigma}^{\dagger}$) denote the QD annihilation (creation) operators, σ refers to spin \uparrow or \downarrow configurations, ε_d is the QD energy level, U_d describes the repulsive Coulomb potential between the opposite spin electrons and $V_{\mathbf{k}\beta}$ is the hybridization of the QD electrons with external reservoirs.

We treat electrons of the metallic reservoir as the free fermion gas $\hat{H}_N = \sum_{\mathbf{k},\sigma} \xi_{\mathbf{k}N} \hat{c}_{\mathbf{k}\sigma N}^\dagger \hat{c}_{\mathbf{k}\sigma N}$ and describe the superconducting electrode by the BCS Hamiltonian $\hat{H}_S = \sum_{\mathbf{k},\sigma} \xi_{\mathbf{k}S} \hat{c}_{\mathbf{k}\sigma S}^\dagger \hat{c}_{\mathbf{k}\sigma S} - \sum_{\mathbf{k}} \Delta \left(\hat{c}_{\mathbf{k}\uparrow S}^\dagger \hat{c}_{-\mathbf{k}\downarrow S}^\dagger + \hat{c}_{-\mathbf{k}\downarrow S} \hat{c}_{\mathbf{k}\uparrow S} \right)$. Energies of mobile electrons $\xi_{\mathbf{k}\beta} = \varepsilon_{\mathbf{k}\beta} - \mu_\beta$ are measured with respect to the chemical potentials μ_β (which can be detuned by voltage V applied across the junction). In this work we focus on the equilibrium condition $\mu_N = \mu_S$ and the central task of our study is the effective low energy physics in a subgap regime $|\omega| < \Delta$. We shall assume the wide band limit approximation $|V_{\mathbf{k}\beta}| \ll D$ (where $-D \leq \varepsilon_{\mathbf{k}\beta} \leq D$) and use the half-bandwidth D as a convenient energy unit. For simplicity we also impose the constant hybridization couplings $\Gamma_\beta \equiv 2\pi \sum_{\mathbf{k}} |V_{\mathbf{k}\beta}|^2 \delta(\omega - \xi_{\mathbf{k}\beta})$.

Deep in the subgap regime $|\omega| \ll \Delta$ the electronic states are affected by the superconducting reservoir merely through the induced on-dot pairing gap Δ_d . It can be shown (more detailed arguments are provided in section I of the supplementary material) that the strong hybridization Γ_S induces the pairing gap $\Delta_d \simeq \Gamma_S/2$ [16]. Microscopic model of the proximized quantum dot can be thus represented by the auxiliary Hamiltonian

$$\begin{aligned} \hat{H} = & \sum_{\mathbf{k}\sigma} \xi_{\mathbf{k}} \hat{c}_{\mathbf{k}\sigma}^\dagger \hat{c}_{\mathbf{k}\sigma} + \sum_{\sigma} \varepsilon_d \hat{d}_{\sigma}^\dagger \hat{d}_{\sigma} - \Delta_d \left(\hat{d}_{\uparrow}^\dagger \hat{d}_{\downarrow}^\dagger + \hat{d}_{\downarrow} \hat{d}_{\uparrow} \right) \\ & + U_d \hat{n}_{d\uparrow} \hat{n}_{d\downarrow} + \frac{1}{\sqrt{N}} \sum_{\mathbf{k}\sigma} V_{\mathbf{k}} \left(\hat{c}_{\mathbf{k}\sigma}^\dagger \hat{d}_{\sigma} + \hat{d}_{\sigma}^\dagger \hat{c}_{\mathbf{k}\sigma} \right). \end{aligned} \quad (1)$$

From now onwards we consider this Hamiltonian (1) trying to determine the effective low energy physics in presence of correlations. Since we have to deal only with the metallic reservoir we can abbreviate the notation by skipping the subindex N in $\xi_{\mathbf{k}N}$, $V_{\mathbf{k}N}$ and $\hat{c}_{\mathbf{k}\sigma,N}^{(\dagger)}$.

Outline of the CUT method – We shall now construct the unitary transformation simplifying the model Hamiltonian (1) to its equivalent easier form. Instead of single step transformation we use the novel method introduced by F. Wegner [21] and independently by K.G. Wilson with S. Głazek [22]. The underlying idea is a continuous transformation $\hat{H}(l) = \hat{U}(l) \hat{H} \hat{U}^{-1}(l)$ which via sequence of infinitesimal steps $l \rightarrow l + \delta l$ transforms the Hamiltonian to the required (diagonal, block-diagonal or any other) structure. Such continuous transformation depends on a specific choice of the operator $\hat{U}(l)$. The transformed Hamiltonian obeys the *flow* equation $\frac{d\hat{H}(l)}{dl} = \frac{d\hat{U}(l)}{dl} \hat{H} \hat{U}^{-1}(l) + \hat{U}(l) \hat{H} \frac{d\hat{U}^{-1}(l)}{dl}$, and due to the identity $\hat{U}(l) \hat{U}^{-1}(l) = 1$ implying $\frac{d\hat{U}(l)}{dl} \hat{U}^{-1}(l) = -\hat{U}(l) \frac{d\hat{U}^{-1}(l)}{dl}$, it can be formally expressed as follows [21]

$$\frac{d\hat{H}(l)}{dl} = [\hat{\eta}(l), \hat{H}(l)] \quad (2)$$

with the generating operator $\hat{\eta}(l) \equiv \frac{d\hat{U}(l)}{dl} \hat{U}^{-1}(l)$.

The differential flow equation (2) enforces scaling (renormalization) of the model parameters (all quantities

become l -dependent). Initially mainly the large energy states are transformed whereas the small energy sector is rescaled later on [23]. This continuous scaling proceeds, however, in the full Hilbert space. We thus keep information about all energy states and can study mutual feedback effects between the large and small energy sectors instead of integrating out 'the fast modes' typical for the RG methods.

The continuous transformation of $\hat{H}(l)$ is controlled via equation (2) by the operator $\hat{\eta}(l)$. It has been shown by Wegner [21] that for Hamiltonian $\hat{H}(l) = \hat{H}_0(l) + \hat{V}(l)$ it is convenient to choose

$$\hat{\eta}(l) = [\hat{H}_0(l), \hat{V}(l)] \quad (3)$$

because (3) guarantees that $\hat{V}(l)$ vanishes in the asymptotic limit $l \rightarrow \infty$. Of course, there are possible also alternative options [23]. Our present study is based on the scheme (3). We would like to remark that CUT method has been already successfully applied to the single impurity Anderson model (in absence of the proximity induced pairing) by S. Kehrein and A. Mielke [24], revisiting the single step Schrieffer-Wolff (S-W) transformation [20]. The authors have shown that the momentum dependent spin-exchange coupling is free of any divergences and close to Fermi surface becomes antiferromagnetic.

The flow equations – We shall formulate a continuous extension of the S-W transformation for the Hamiltonian (1) using the choice (3) in order to eliminate the hybridization term $\hat{V}(l) = \frac{1}{\sqrt{N}} \sum_{\mathbf{k}\sigma} V_{\mathbf{k}}(l) \left(\hat{c}_{\mathbf{k}\sigma}^\dagger \hat{d}_{\sigma} + \hat{d}_{\sigma}^\dagger \hat{c}_{\mathbf{k}\sigma} \right)$. During this process the parameters of $\hat{H}_0(l) \equiv \hat{H}(l) - \hat{V}(l)$ are renormalized and some additional terms become generated (see section II of the Supplementary material). The generating operator (3) has antihermitean structure $\hat{\eta}(l) = \hat{\eta}_0(l) - \hat{\eta}_0^\dagger(l)$, where

$$\begin{aligned} \hat{\eta}_0(l) = & \sum_{\mathbf{k}\sigma} \left(\eta_{\mathbf{k}}(l) + \eta_{\mathbf{k}}^{(2)}(l) \hat{d}_{-\sigma}^\dagger \hat{d}_{-\sigma} \right) \hat{c}_{\mathbf{k}\sigma}^\dagger \hat{d}_{\sigma} \\ & + \sum_{\mathbf{k}\mathbf{p}\sigma} \eta_{\mathbf{k}\mathbf{p}}(l) \hat{c}_{\mathbf{k}\sigma}^\dagger \hat{c}_{\mathbf{p}\sigma} + \sum_{\mathbf{k}} \eta_{\mathbf{k}}^{(1)}(l) \left(\hat{c}_{\mathbf{k}\uparrow}^\dagger \hat{d}_{\downarrow}^\dagger - \hat{c}_{\mathbf{k}\downarrow}^\dagger \hat{d}_{\uparrow}^\dagger \right) \end{aligned} \quad (4)$$

and l -dependent coefficients are given by $\eta_{\mathbf{k}}(l) = \frac{1}{\sqrt{N}} (\xi_{\mathbf{k}}(l) - \varepsilon_d(l)) V_{\mathbf{k}}(l)$, $\eta_{\mathbf{k}\mathbf{p}}(l) = \frac{1}{N} V_{\mathbf{k}}(l) V_{\mathbf{p}}(l)$, $\eta_{\mathbf{k}}^{(1)}(l) = \frac{1}{\sqrt{N}} \Delta_d(l) V_{\mathbf{k}}(l)$, $\eta_{\mathbf{k}}^{(2)}(l) = -\frac{1}{\sqrt{N}} U(l) V_{\mathbf{k}}(l)$. Let us remark that the standard S-W transformation $e^{\hat{S}} \hat{H} e^{-\hat{S}}$ [20] can be reproduced with the operator \hat{S} of the same structure as (4) using $\eta_{\mathbf{k}} = \frac{1}{\sqrt{N}} V_{\mathbf{k}} / (\xi_{\mathbf{k}} - \varepsilon_d)$, $\eta_{\mathbf{k}}^{(2)} = \frac{1}{\sqrt{N}} V_{\mathbf{k}} U / [(\varepsilon_d - \xi_{\mathbf{k}})(\varepsilon_d + U - \xi_{\mathbf{k}})]$ and $\eta_{\mathbf{k}}^{(1)} = 0 = \eta_{\mathbf{k}\mathbf{p}}$. This fact indicates common roots of the single step and continuous transformation for a given problem at hand.

Substituting (4) to the right h.s of the flow equation (2) we obtain some terms, which initially were absent in the model Hamiltonian (1). From these new contributions we take here into account only the spin-exchange interactions, essential for the Kondo physics

(but this procedure can be easily extended on other interactions). We update the initial Hamiltonian (1) by $H_{exch}(l) = -\sum_{\mathbf{k},\mathbf{p}} J_{\mathbf{k}\mathbf{p}}(l) \hat{\mathbf{s}}_d \cdot \hat{\mathbf{S}}_{\mathbf{k}\mathbf{p}}$ with the boundary constraint $J_{\mathbf{k}\mathbf{p}}(0) = 0$. Spin operator of the QD is denoted by $\hat{\mathbf{s}}_d$ and $\hat{\mathbf{S}}_{\mathbf{k}\mathbf{p}}$ describes spins of mobile electrons of the metallic lead. From the lengthy but straightforward algebra (see the section II.b of the supplementary material) we derive the following set of coupled *flow equations*

$$\frac{d\varepsilon_d(l)}{dl} = -\frac{2}{\sqrt{N}} \sum_{\mathbf{k}} \eta_{\mathbf{k}}(l) V_{\mathbf{k}}(l), \quad (5)$$

$$\frac{dU_d(l)}{dl} = -\frac{4}{\sqrt{N}} \sum_{\mathbf{k}} \eta_{\mathbf{k}}^{(2)}(l) V_{\mathbf{k}}(l), \quad (6)$$

$$\frac{d\Delta_d(l)}{dl} = \frac{2}{\sqrt{N}} \sum_{\mathbf{k}} \eta_{\mathbf{k}}^{(1)}(l) V_{\mathbf{k}}(l), \quad (7)$$

$$\begin{aligned} \frac{dV_{\mathbf{k}}(l)}{dl} &= \eta_{\mathbf{k}}(l) [\varepsilon_d(l) - \xi_{\mathbf{k}}(l) + U_d(l) \langle \hat{n}_{d,\sigma} \rangle] \\ &+ \frac{2}{\sqrt{N}} \sum_{\mathbf{p}} \eta_{\mathbf{k}\mathbf{p}}(l) V_{\mathbf{p}}(l) - \eta_{\mathbf{k}}^{(1)}(l) \Delta_d(l) \\ &+ \eta_{\mathbf{k}}^{(2)}(l) [\varepsilon_d(l) - \xi_{\mathbf{k}}(l) + U_d(l)] \langle \hat{n}_{d,\sigma} \rangle, \\ \frac{dJ_{\mathbf{k}\mathbf{p}}(l)}{dl} &= \eta_{\mathbf{k}}^{(2)}(l) V_{\mathbf{p}}(l) + \eta_{\mathbf{p}}^{(2)}(l) V_{\mathbf{k}}(l) \\ &- (\xi_{\mathbf{k}} - \xi_{\mathbf{p}})^2 J_{\mathbf{k}\mathbf{p}}(l). \end{aligned} \quad (8)$$

We skipped the derivative $\frac{d}{dl} \xi_{\mathbf{k}}(l)$ because it vanishes in the thermodynamic limit $N \rightarrow \infty$, implying $\xi_{\mathbf{k}}(l) = \xi_{\mathbf{k}}$.

Lowest order estimation – To gain some analytical (although approximate) solution of the flow equations (5-9) we use the lowest order iterative estimation, justified for $V_{\mathbf{k}} \ll D$. In the first step we estimate $V_{\mathbf{k}}(l)$ solving the equation (8) upon neglecting l -dependence of all other parameters. To simplify such analysis we restrict to the half-filled quantum dot case $n_{d\sigma} = 0.5$ (i.e. $\varepsilon_d = -U_d/2$). Neglecting the cubic term $\eta_{\mathbf{k}\mathbf{p}}(l) V_{\mathbf{p}}(l)$ in (8) we obtain

$$V_{\mathbf{k}}(l) = V_{\mathbf{k}} \exp[-f_{\mathbf{k}} l], \quad (10)$$

where $f_{\mathbf{k}} \equiv (\varepsilon_d - \xi_{\mathbf{k}})^2 + \Delta_d^2 + (\varepsilon_d + U_d/2 - \xi_{\mathbf{k}}) U_d$. This expression (10) yields an exponential disappearance of the hybridization coupling $V_{\mathbf{k}}(l)$. In the next step way can estimate l -dependence of all other quantities. Since we are particularly interested in the spin interactions we provide explicit expression only for the exchange coupling

$$J_{\mathbf{k}\mathbf{p}}(l) = \frac{-2U_d V_{\mathbf{k}} V_{\mathbf{p}}}{f_{\mathbf{k}} + f_{\mathbf{p}} - (\xi_{\mathbf{k}} - \xi_{\mathbf{p}})^2} \left[1 - e^{-(f_{\mathbf{k}} + f_{\mathbf{p}})l} \right]. \quad (11)$$

Nearby the Fermi surface (when $\xi_{\mathbf{k}_F} = 0 = \xi_{\mathbf{p}_F}$) the exchange coupling (11) becomes negative (antiferromagnetic), approaching the following asymptotic value

$$J_{\mathbf{k}_F \mathbf{p}_F}(l \rightarrow \infty) = \frac{-4U_d |V_{\mathbf{k}_F}|^2}{U_d^2 + (2\Delta_d)^2}. \quad (12)$$

Let us compare this result (12) to the value $-4|V_{\mathbf{k}_F}|^2/U_d$ obtained previously from the S-W [20] and the CUT

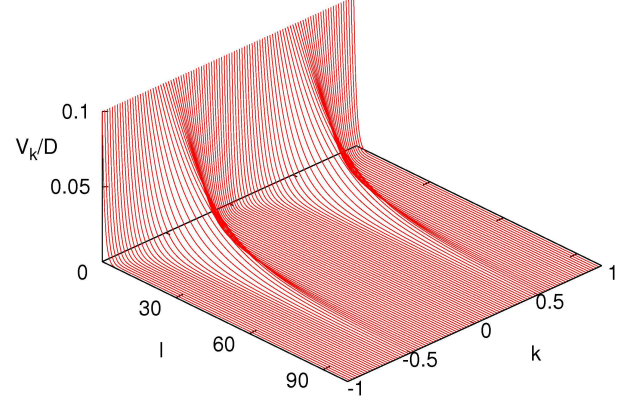


FIG. 1: (color online) Flow of the hybridization coupling $V_{\mathbf{k}}(l)$ obtained for the initial values of the model (1) parameters: $\varepsilon_d/D = -0.2$, $U_d/D = 0.4$, $\Delta_d/D = 0.1$ and $V_{\mathbf{k}}/D = 0.1$.

study [24] for the half-filled Anderson impurity embedded in a metallic medium. We notice that the proximity induced on-dot pairing Δ_d substantially weakens the exchange coupling.

Numerical solution – To check the validity of our analytical results we solved the flow equations (5-9) fully self-consistently, implementing the numerical Runge-Kutta algorithm. For the computations we discretized the energy band $\xi_{\mathbf{k}}/D = -1 + 2|k|$ by a mesh of 1000 equidistant points $k \in [-1, 1]$. For the half-filled QD the Fermi level $\xi_{\mathbf{k}_F} = 0$ corresponds to $|k| = 0.5$. We carried out the calculations for small hybridization dot case $n_{d\sigma} = 0.5$. All l -dependent quantities were determined from the following iterative scheme $x(l + \delta l) \simeq x(l) + x'(l)\delta l$ with derivative $x'(l)$ taken from the flow equations (5-9). We changed the increment δl , depending on a magnitude the continuous parameter l . At initial steps of the transformation we used $\delta l = 0.01$ (for $0 \leq l < 1$) and gradually increased it for higher values of l (these values are expressed in units D^{-2}). We continued the numerical procedure calculating all l -dependent quantities up to $l = 100$, when $V_{\mathbf{k}}(l)$ decreased more than 6 orders from its initial value.

Figure 1 shows variation of the hybridization coupling $V_{\mathbf{k}}(l)$ with respect to the flow parameter l . We clearly see that it vanishes, roughly obeying the exponential relation (10). Hybridization of the electronic states distant from the Fermi level are transformed pretty fast, whereas the states closer nearby the Fermi momentum $k_F = \pm 0.5$ are eliminated later on. This procedure resembles integrating out the fast and slow energy modes by the numerical renormalization group methods.

Exponential decrease of $V_{\mathbf{k}}(l)$ is accompanied by ongoing renormalization of the QD energy $\varepsilon_d(l)$, Coulomb interaction $U_d(l)$ and the pairing gap $\Delta_d(l)$. Since we assumed the hybridization to be small therefore these renormalizations proved to be rather marginal (figure 2).

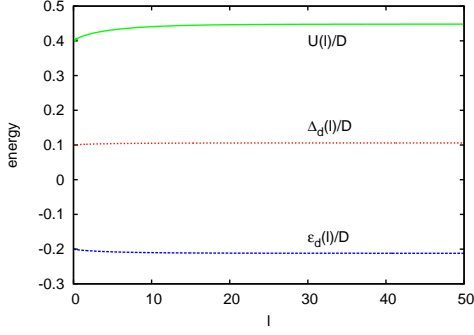


FIG. 2: (color online) Variation of the quantum dot energy $\varepsilon_d(l)$, Coulomb repulsion $U_d(l)$, and the on-dot pairing $\Delta_d(l)$ with respect to l for the same set of parameters as in fig. 1.

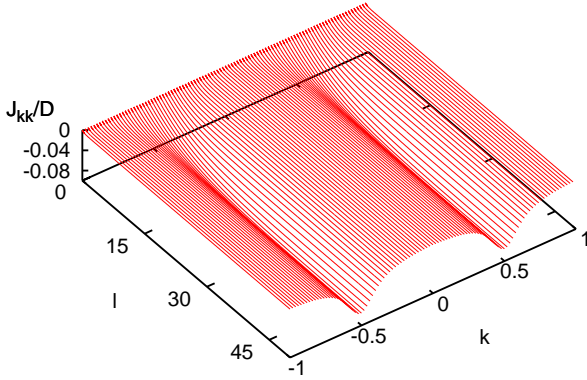


FIG. 3: (color online) The spin exchange coupling $J_{\mathbf{k}\mathbf{p}}(l)$ obtained for the same set of parameters as in figure 2. For illustration we choose $\mathbf{k} = \mathbf{p}$, when the exchange coupling is negative (otherwise $J_{\mathbf{k}\neq\mathbf{p}}(l)$ changes the sign for momenta distant from the Fermi surface).

The most important physical result is the induced spin-exchange coupling $J_{\mathbf{k}\mathbf{p}}(l)$. Figure 3 illustrates its l -dependence obtained for $\mathbf{k} = \mathbf{p}$. We can notice the negative (antiferromagnetic) coupling which is strongly enhanced nearby the Fermi surface, in agreement with (11). We repeated the selfconsistent numerical calculations for a number of Δ_d values. The effective (asymptotic limit) value $J_{\mathbf{k}_F\mathbf{p}_F}(l = \infty)$ is shown by points in figure 4. For comparison we also plot the analytical value (solid line). The analytical formula (12) overestimates $J_{\mathbf{k}_F\mathbf{p}_F}(l = \infty)$ by a few percent. Summarizing, we conclude that the induced on-dot pairing has a detrimental influence on the antiferromagnetic coupling. To get some insight into the Kondo temperature T_K we estimate its value from the Bethe-ansatz formula [25] $k_B T_K = \frac{2}{\pi} D \exp \{ -\phi [2\rho(\varepsilon_F) J_{\mathbf{k}_F\mathbf{p}_F}(l = \infty)] \}$, where $\rho(\varepsilon_F)$ is the density of states at the Fermi level and

$\phi(y) \simeq |y|^{-1} - 0.5 \ln |y|$. The obtained Kondo temperature is plotted by dashed line in figure 4. We notice

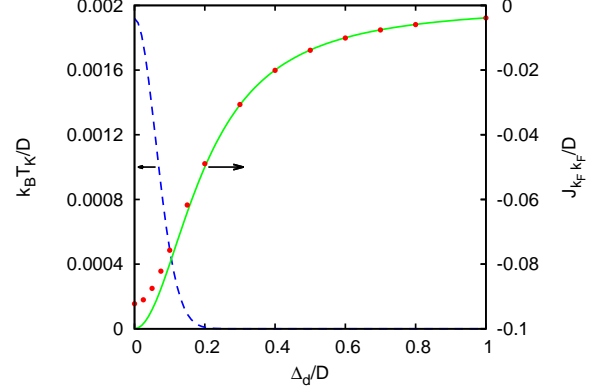


FIG. 4: The asymptotic limit $l \rightarrow \infty$ value of the effective exchange coupling $J_{\mathbf{k}_F\mathbf{k}_F}$ as a function of the on-dot energy gap Δ_d obtained for the symmetric Anderson impurity with the following (initial) parameters: $V_{\mathbf{k}}/D = 0.1$, $\varepsilon_d/D = -0.2$ and $U = -2\varepsilon_d$. The results based on the lowest order estimation (12) (solid line) nearly coincide with the fully selfconsistent numerical solution (points). The dashed curve shows the corresponding Kondo temperature $k_B T_K$.

that T_K is strongly suppressed by the on-dot pairing Δ_d , reproducing qualitatively the experimental results [2].

Summary and outlook – We have investigated the correlated quantum dot coupled between the superconducting and metallic reservoirs. Using the continuous unitary transformation we have determined the effective spin-exchange coupling between the QD and metallic electrons. At the Fermi level such interactions have antiferromagnetic character which is necessary for inducing the Kondo effect. Our approximate analytical formula (12) and the fully selfconsistent numerical solution of the flow equations show that the on-dot pairing Δ_d substantially weakens such antiferromagnetic exchange coupling. In consequence, the Kondo temperature is strongly suppressed by the induced on-dot pairing. This behavior has been indeed observed experimentally (where effective pairing gap was modified by the magnetic field) [2].

Further extension of the present study could be worthwhile for the nonequilibrium situation $\mu_N \neq \mu_S$. To calculate the charge current (of the Andreev and other channels) one can adopt the scheme formulated for the QD coupled between both metallic leads [26]. Besides considering the many-body phenomena under nonequilibrium conditions [27] it could be also interesting to extend the present study to multiterminal configurations with the superconducting electrodes, where electrons released from the Cooper pairs preserve entanglement.

We acknowledge discussions with R. Aguado, J. Bauer, V. Janiš, S. Kehrein, T. Novotný, and K.I. Wysokiński.

-
- [1] R.S. Deacon, Y. Tanaka, A. Oiwa, R. Sakano, K. Yoshida, K. Shibata, K. Hirakawa, and S. Tarucha, *Phys. Rev. Lett.* **104**, 076805 (2010); R.S. Deacon, Y. Tanaka, A. Oiwa, R. Sakano, K. Yoshida, K. Shibata, K. Hirakawa, and S. Tarucha, *Phys. Rev. B* **81**, 121308(R) (2010).
- [2] E.J.H. Lee, X. Jiang, R. Aguado, G. Katsaros, C.M. Lieber, and S. De Franceschi, *Phys. Rev. Lett.* **109**, 186802 (2012).
- [3] E.J.H. Lee, X. Jiang, M. Houzet, R. Aguado, Ch.M. Lieber, S. De Franceschi, *Nature Nanotechnology* **9**, 79 (2014).
- [4] J.D. Pillet, P. Joyez, R. Žitko, and F.M. Goffman, *Phys. Rev. B* **88**, 045101 (2013).
- [5] J. Schindele, A. Baumgartner, R. Maurand, M. Weiss, and C. Schönenberger, arXiv:1311.0659 (preprint).
- [6] J.-D. Pillet, C.H.L. Quay, P. Morfin, C. Bena, A. Levy-Yeyati, and P. Joyez, *Nature Phys.* **6**, 965 (2010).
- [7] T. Dirks, T.L. Hughes, S. Lal, B. Uchoa, Y.-F. Chen, C. Chialvo, P.M. Golbart, and N. Mason, *Nature Phys.* **7**, 386 (2011).
- [8] L. Bretheau, C.Ö. Girit, H. Pothier, D. Esteve, and C. Urbina, *Nature* **499**, 312 (2013).
- [9] H.I. Jørgensen, T. Novotný, K. Grove-Rasmussen, K. Flensberg, and P.E. Lindelof, *Nano Lett.* **7**, 2441 (2007).
- [10] M. Pustilnik and L.I. Glazman, *J. Phys.: Condens. Matter* **16**, R513 (2004).
- [11] J. Bauer, A. Oguri, and A.C. Hewson, *J. Phys.: Condens. Matter* **19**, 486211 (2007).
- [12] R. Maurand, Ch. Schönenberger, *Physics* **6**, 75 (2013).
- [13] A. Martín-Rodero and A. Levy-Yeyati, *Adv. Phys.* **60**, 899 (2011).
- [14] Y. Yamada, Y. Tanaka, and N. Kawakami, *Phys. Rev. B* **84**, 075484 (2011); A. Oguri, Y. Tanaka, and J. Bauer, *Phys. Rev. B* **87**, 075432 (2013).
- [15] R. Fazio and R. Raimondi, *Phys. Rev. Lett.* **80**, 2913 (1998); *ibid.*, *Phys. Rev. Lett.* **82**, 4950 (1999); K. Kang, *Phys. Rev. B* **58**, 9641 (1998); P. Schwab and R. Raimondi, *Phys. Rev. B* **59**, 1637 (1999); S.Y. Cho, K. Kang, and C.-M. Ryu, *Phys. Rev. B* **60**, 16874 (1999); Q.-F. Sun, J. Wang, and T.-H. Lin, *Phys. Rev. B* **59**, 3831 (1999); A.A. Clerk, V. Ambegaokar, and S. Hershfield, *Phys. Rev. B* **61**, 3555 (2000); Q.-F. Sun, H. Guo, and T.-H. Lin, *Phys. Rev. Lett.* **87**, 176601 (2001). J.C. Cuevas, A. Levy Yeyati, and A. Martín-Rodero, *Phys. Rev. B* **63**, 094515 (2001); Y. Avishai, A. Golub, and A.D. Zaikin, *Phys. Rev. B* **63**, 134515 (2001); Y. Avishai, A. Golub, and A.D. Zaikin, *Phys. Rev. B* **67**, 041301(R) (2003); M. Krawiec and K.I. Wysokiński, *Supercond. Sci. Technol.* **17**, 103 (2004); Y. Tanaka, N. Kawakami, and A. Oguri, *J. Phys. Soc. Jpn.* **76**, 074701 (2007); C. Karrasch, A. Oguri, and V. Meden, *Phys. Rev. B* **77**, 024517 (2008); C. Karrasch and V. Meden, *Phys. Rev. B* **79**, 045110 (2009); D. Futturrer, M. Governale, and J. König, *EPL* **91**, 47004 (2010); T. Meng, S. Florens, and P. Simon, *Phys. Rev. B* **79**, 224521 (2010); V. Koerting, B.M. Andersen, K. Flensberg, and J. Paaske, *Phys. Rev. B* **82**, 245108 (2010); B.M. Andersen, K. Flensberg, V. Koerting, and J. Paaske, *Phys. Rev. Lett.* **107**, 256802 (2011); D. Futturrer, J. Świebodziński, M. Governale, and J. König, *Phys. Rev. B* **87**, 014509 (2013); A. Koga, *Phys. Rev. B* **87**, 115409 (2013); J. Bauer, J.I. Pascual, and K.J. Franke, *Phys. Rev. B* **87**, 075125 (2013).
- [16] J. Barański and T. Domański, *J. Phys.: Condens. Matter* **25**, 435305 (2013); T. Domański and A. Donabidowicz, *Phys. Rev. B* **78**, 073105 (2008); T. Domański, A. Donabidowicz, and K.I. Wysokiński, *Phys. Rev. B* **78**, 144515 (2008); *ibid.* *Phys. Rev. B* **76**, 104514 (2007).
- [17] W. Chang, V.E. Manucharyan, T.S. Jespersen, J. Nygård, and C.M. Marcus, *Phys. Rev. Lett.* **110**, 217005 (2013).
- [18] F. Hübner, M.J. Wolf, T. Scherer, D. Wang, D. Beckmann, and H. v. Löhneysen, *Phys. Rev. Lett.* **109**, 087004 (2012).
- [19] V. Mourik, K. Zuo, S.M. Frolov, S.R. Plissard, E.P.A.M. Bakkers, and L.P. Kouwenhoven, *Science* **336**, 1003 (2012); A. Das, Y. Ronen, Y. Most, Y. Oreg, M. Heiblum, and H. Shtrikman, *Nature Phys.* **8**, 887 (2012); M.T. Dengh, C.L. Yu, G.Y. Huang, M. Larsson, P. Caroff, and H.Q. Xu, *Nanoletters* **12**, 6414 (2012).
- [20] J.R. Schrieffer, P.A. Wolff, *Phys. Rev.* **149**, 491 (1966).
- [21] F. Wegner, *Ann. Physik (Leipzig)* **3**, 77 (1994).
- [22] S.D. Glazek, K.G. Wilson, *Phys. Rev. D* **49**, 4214 (1994).
- [23] S. Kehrein, *The flow equation approach to many-particle systems*, (Springer Tracts in Modern Physics **215**, Berlin, 2006).
- [24] S. Kehrein and A. Mielke, *J. Phys. A: Math. Gen.* **27**, 4259 (1994); S. Kehrein and A. Mielke, *Ann. Phys.* **252**, 1 (1996).
- [25] A.M. Tsvelick and P.B. Wiegmann, *Adv. Phys.* **32**, 453 (1983).
- [26] P. Fritsch, S. Kehrein, *Phys. Rev. B* **81**, 035113 (2010); P. Wang and S. Kehrein, *Phys. Rev. B* **82**, 125124 (2010).
- [27] S. Kehrein, *Phys. Rev. Lett.* **95**, 056602 (2005); C. Tomaras and S. Kehrein, *EPL* **93**, 47011 (2011); H. Krull, N.A. Drescher, G.S. Uhrig, *Phys. Rev. B* **86**, 125113 (2012); B. Fauseweh and G.S. Uhrig, *Phys. Rev. B* **87**, 184406 (2013); A. Verdeny, A. Mielke, and F. Mintert, *Phys. Rev. Lett.* **111**, 175301 (2013); M. Heyl, A. Polkovnikov, and S. Kehrein, *Phys. Rev. Lett.* **110**, 135704 (2013); M. Medvedyeva, A. Hoffmann, and S. Kehrein, *Phys. Rev. B* **88**, 094306 (2013).

Supplementary material to 'Kondo impurity between superconducting and metallic reservoir: the flow equation approach'

M. Zapalska and T. Domański

Institute of Physics, M. Curie Skłodowska University, 20-031 Lublin, Poland

(Dated: February 7, 2014)

I. HAMILTONIAN OF PROXIMIZED QD

For microscopic description of the N-QD-S heterojunction we can use the Anderson-type Hamiltonian

$$\hat{H} = \sum_{\beta} \hat{H}_{\beta} + \sum_{\sigma} \epsilon_d \hat{d}_{\sigma}^{\dagger} \hat{d}_{\sigma} + U_d \hat{n}_{d\uparrow} \hat{n}_{d\downarrow} \quad (1)$$

$$+ \sum_{\mathbf{k}, \sigma} \sum_{\beta} \left(V_{\mathbf{k}\beta} \hat{d}_{\sigma}^{\dagger} \hat{c}_{\mathbf{k}\sigma\beta} + V_{\mathbf{k}\beta}^{*} \hat{c}_{\mathbf{k}\sigma\beta}^{\dagger} \hat{d}_{\sigma} \right),$$

where the subindex β refers either to the normal metal (N) or the superconducting (S) electrode. Reservoirs of such itinerant electrons can be represented correspondingly by the Hamiltonian of a free Fermi gas $\hat{H}_N = \sum_{\mathbf{k}, \sigma} \xi_{\mathbf{k}N} \hat{c}_{\mathbf{k}\sigma N}^{\dagger} \hat{c}_{\mathbf{k}\sigma N}$ and the usual BCS form $\hat{H}_S = \sum_{\mathbf{k}, \sigma} \xi_{\mathbf{k}S} \hat{c}_{\mathbf{k}\sigma S}^{\dagger} \hat{c}_{\mathbf{k}\sigma S} - \sum_{\mathbf{k}} \Delta \left(\hat{c}_{\mathbf{k}\uparrow S}^{\dagger} \hat{c}_{-\mathbf{k}\downarrow S}^{\dagger} + \hat{c}_{-\mathbf{k}\downarrow S} \hat{c}_{\mathbf{k}\uparrow S} \right)$.

The qualitative features originating from the proximity effect can be deduced by studying the single particle Green's function $\mathbf{G}_d(\tau, \tau') = \langle \langle \hat{\Psi}_d(\tau); \hat{\Psi}_d^{\dagger}(\tau') \rangle \rangle$ in the Nambu spinor representation $\hat{\Psi}_d^{\dagger} = (\hat{d}_{\uparrow}^{\dagger}, \hat{d}_{\downarrow}^{\dagger})$, $\hat{\Psi}_d = (\hat{\Psi}_d^{\dagger})^{\dagger}$. In absence of an external voltage the Green's function $\mathbf{G}_d(\tau, \tau')$ depends only on time difference $\tau - \tau'$ and its Fourier transform obeys

$$[\mathbf{G}_d(\omega)]^{-1} = \begin{pmatrix} \omega - \epsilon_d & 0 \\ 0 & \omega + \epsilon_d \end{pmatrix} - \Sigma_d^0(\omega) - \Sigma_d^U(\omega). \quad (2)$$

The first contribution Σ_d^0 takes into account the hybridization effects (of an uncorrelated quantum impurity) whereas the second part Σ_d^U describes the corrections due to the Coulomb repulsion U_d .

The hybridization part $\Sigma_d^0(\omega)$ is known exactly. Its explicit form for the wide-band limit is found as [1]

$$\Sigma_d^0(\omega) = -\frac{\Gamma_N}{2} \begin{pmatrix} i & 0 \\ 0 & i \end{pmatrix} \quad (3)$$

$$- \frac{\Gamma_S}{2} \begin{pmatrix} 1 & \frac{\Delta}{\omega} \\ \frac{\Delta}{\omega} & 1 \end{pmatrix} \times \begin{cases} \frac{\omega}{\sqrt{\Delta^2 - \omega^2}} & \text{for } |\omega| < \Delta, \\ \frac{i|\omega|}{\sqrt{\omega^2 - \Delta^2}} & \text{for } |\omega| > \Delta. \end{cases}$$

Roughly speaking, the selfenergy $\Sigma_d^0(\omega)$ is responsible for: a) the induced on-dot pairing (due to off-diagonal terms which are proportional to Γ_S) and b) the finite life-time effects (i.e. broadening of the QD states). The latter effect depends either on both couplings $\Gamma_{\beta=N,S}$ (for energies $|\omega| \geq \Delta$) or solely on Γ_N (in a subgap regime $|\omega| < \Delta$). Figure 1 illustrates the typical spectral function $\rho_d(\omega) = -\pi^{-1} \text{Im} \mathbf{G}_d(\omega + i0^+)$ obtained for the uncorrelated ($U_d = 0$) quantum dot.

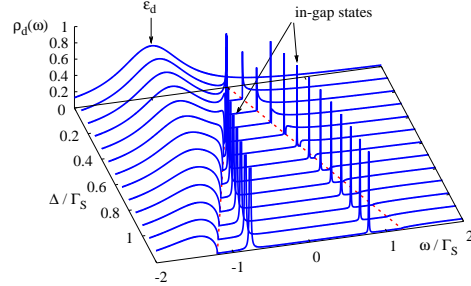


FIG. 1: Spectral function $\rho_d(\omega)$ of the uncorrelated quantum dot obtained for $\epsilon_d/\Gamma_S = -1$ assuming a strong asymmetry of the hybridization $\Gamma_N/\Gamma_S = 10^{-3}$. We can notice that the in-gap (Andreev) quasiparticles emerge from the singularities $\pm\Delta$ (dashed lines) and gradually evolve to $\pm\sqrt{\epsilon_d^2 + (\Gamma_S/2)^2}$. For arbitrary parameters they appear symmetrically around the Fermi level (chosen here as $\omega = 0$).

In a subgap regime $|\omega| < \Delta$ the single particle Green's function of the uncorrelated quantum dot has the BCS-type structure

$$\mathbf{G}_d(\omega) = \begin{pmatrix} \tilde{\omega} + \epsilon_d + i\Gamma_N/2 & \tilde{\Gamma}_s/2 \\ \tilde{\Gamma}_s/2 & \tilde{\omega} - \epsilon_d + i\Gamma_N/2 \end{pmatrix}^{-1} \quad (4)$$

with $\tilde{\omega} = \omega + \frac{\Gamma_S}{2} \frac{\omega}{\sqrt{\Delta^2 - \omega^2}}$ and $\tilde{\Gamma}_s = \Gamma_S \frac{\Delta}{\sqrt{\Delta^2 - \omega^2}}$. The subgap spectrum is thus characterized by two quasiparticle peaks, widely known in the literature as the Andreev [1] or Shiba-Rusinov [2] states. Let us emphasize that they originate from the induced on-dot pairing.

For infinitesimally small coupling Γ_N the in-gap spectrum consists of the Dirac-deltas (corresponding to the long-lived quasiparticles). Otherwise the Andreev states acquire some finite broadening, roughly controlled by the hybridization Γ_N . The quasiparticle energies $E_{A,\pm}$ of the uncorrelated quantum dot can be determined from the following relation [3]

$$E_{A,\pm} + \frac{(\Gamma_S/2)E_{A,\pm}}{\sqrt{\Delta^2 - E_{A,\pm}^2}} = \pm \sqrt{\epsilon_d^2 + \frac{(\Gamma_S/2)^2 \Delta^2}{\Delta^2 - E_{A,\pm}^2}}. \quad (5)$$

In figure 2 we plot these quasiparticle energies $E_{A,\pm}$ versus the superconducting gap Δ for $\epsilon_d/\Gamma_S = -1$, $U_d = 0$, $\Gamma_N \ll \Gamma_S$. In the limit $\Delta \ll \Gamma_S$ the Andreev states are located close-by the gap edge singularities $E_{A,\pm} \simeq \pm\Delta$. In the other extreme limit $\Delta \gg \Gamma_S$ they asymptotically approach $E_{A,\pm} \simeq \pm\sqrt{\epsilon_d^2 + (\Gamma_S/2)^2}$. In the latter

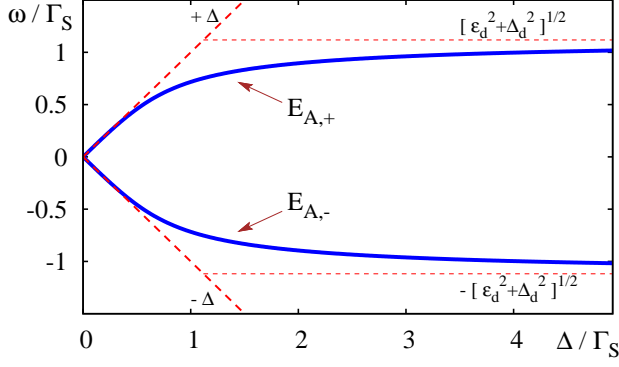


FIG. 2: Energies $E_{A,\pm}$ of the subgap (Andreev) quasiparticles for the same set of parameters as in figure 1.

case (known as *the superconducting atomic limit*) the hybridization selfenergy (3) simplifies to the static value

$$\Sigma_d^0(\omega) = -\frac{1}{2} \begin{pmatrix} i\Gamma_N & \Gamma_S \\ \Gamma_S & i\Gamma_N \end{pmatrix}. \quad (6)$$

One can hence replace the initial Hamiltonian (1) by its equivalent version

$$\begin{aligned} \hat{H} = & \sum_{\sigma} \epsilon_d \hat{d}_{\sigma}^{\dagger} \hat{d}_{\sigma} + U_d \hat{n}_{d\uparrow} \hat{n}_{d\downarrow} - \left(\Delta_d \hat{d}_{\uparrow}^{\dagger} \hat{d}_{\downarrow}^{\dagger} + \text{h.c.} \right) \\ & + \hat{H}_N + \sum_{\mathbf{k}, \sigma} \left(V_{\mathbf{k}N} \hat{d}_{\sigma}^{\dagger} \hat{c}_{\mathbf{k}\sigma N} + V_{\mathbf{k}N}^* \hat{c}_{\mathbf{k}\sigma N}^{\dagger} \hat{d}_{\sigma} \right), \end{aligned} \quad (7)$$

where a role of the superconducting electrode is played by the induced on-dot gap $\Delta_d = \Gamma_S/2$.

II. CONTINUOUS S-W TRANSFORMATION

In this section we present some details on the continuous Schrieffer-Wolf transformation $\hat{H}(l) = \hat{\mathcal{U}}(l) \hat{H} \hat{\mathcal{U}}^{\dagger}(l)$ for the Hamiltonian (7). Here and in the main text of the paper we abbreviate the notation skipping the subindex N in $V_{\mathbf{k}N}$ and $\xi_{\mathbf{k}N}$. We are going to construct such unitary transformation $\hat{\mathcal{U}}(l)$ eliminating the hybridization term $\hat{V}(l) = \sum_{\mathbf{k}, \sigma} \left(V_{\mathbf{k}}(l) \hat{d}_{\sigma}^{\dagger} \hat{c}_{\mathbf{k}\sigma} + V_{\mathbf{k}}^*(l) \hat{c}_{\mathbf{k}\sigma}^{\dagger} \hat{d}_{\sigma} \right)$ in the asymptotic limit $\lim_{l \rightarrow \infty} V_{\mathbf{k}}(l) = 0$.

A. The generating operator

To derive the effective Hamiltonian $\hat{H}(l \rightarrow \infty)$ we follow strictly the method introduced by Wegner [5]. Evolution of the Hamiltonian has to be derived from the formal differential equation

$$\frac{d\hat{H}(l)}{dl} = [\hat{\eta}(l), \hat{H}(l)], \quad (8)$$

where the generating operator is defined by $\hat{\eta}(l) \equiv \frac{d\hat{\mathcal{U}}(l)}{dl} \hat{\mathcal{U}}^{-1}(l)$. According to Ref. [5] one possible way for choosing $\hat{\eta}(l)$ is

$$\hat{\eta}(l) = [\hat{H}(l), \hat{V}(l)] \quad (9)$$

although also other alternative options are available [6]. For the considered Hamiltonian (7) the canonical operator $\hat{\eta}(l)$ has the explicit form

$$\begin{aligned} \hat{\eta}(l) = & \sum_{\mathbf{k}\sigma} \left(\eta_{\mathbf{k}}(l) \hat{c}_{\mathbf{k}\sigma}^{\dagger} \hat{d}_{\sigma} - \text{h.c.} \right) \\ & + \sum_{\mathbf{k}\mathbf{p}\sigma} \left(\eta_{\mathbf{k}\mathbf{p}}(l) \hat{c}_{\mathbf{k}\sigma}^{\dagger} \hat{c}_{\mathbf{p}\sigma} - \text{h.c.} \right) \\ & + \sum_{\mathbf{k}} \left(\eta_{\mathbf{k}}^{(1)}(l) \left(\hat{c}_{\mathbf{k}\uparrow}^{\dagger} \hat{d}_{\downarrow}^{\dagger} - \hat{c}_{\mathbf{k}\downarrow}^{\dagger} \hat{d}_{\uparrow}^{\dagger} \right) - \text{h.c.} \right) \\ & + \sum_{\mathbf{k}\sigma} \eta_{\mathbf{k}}^{(2)}(l) \left(\hat{c}_{\mathbf{k}\sigma}^{\dagger} \hat{d}_{-\sigma}^{\dagger} \hat{d}_{-\sigma} \hat{d}_{\sigma} - \text{h.c.} \right) \end{aligned} \quad (10)$$

with the following l -dependent coefficients $\eta_{\mathbf{k}}(l) = \frac{1}{\sqrt{N}} (\xi_{\mathbf{k}}(l) - \varepsilon_d(l)) V_{\mathbf{k}}(l)$, $\eta_{\mathbf{k}\mathbf{p}}(l) = \frac{1}{N} V_{\mathbf{k}}(l) V_{\mathbf{p}}(l)$, $\eta_{\mathbf{k}}^{(1)}(l) = \frac{1}{\sqrt{N}} \Delta_d(l) V_{\mathbf{k}}(l)$ and $\eta_{\mathbf{k}}^{(2)}(l) = -\frac{1}{\sqrt{N}} U(l) V_{\mathbf{k}}(l)$. Previous studies [4] of the usual Anderson impurity Hamiltonian (i.e. $\Delta_d = 0$) have been done using the same generating operator (10) without the coefficient $\eta_{\mathbf{k}}^{(1)}(l)$.

B. Derivation of the flow equations

Substituting (10) to the flow equation (8) for the model Hamiltonian (7) one obtains

$$\begin{aligned} [\hat{\eta}(l), \hat{H}(l)] = & \frac{1}{\sqrt{N}} \sum_{\mathbf{k}\mathbf{p}\sigma} \eta_{\mathbf{k}}^{(2)}(l) V_{\mathbf{p}}(l) \left(\hat{c}_{\mathbf{k}\sigma}^{\dagger} \hat{d}_{-\sigma}^{\dagger} \hat{d}_{-\sigma} \hat{c}_{\mathbf{p}\sigma} - \hat{c}_{\mathbf{k}\sigma}^{\dagger} \hat{d}_{-\sigma}^{\dagger} \hat{d}_{\sigma} \hat{c}_{\mathbf{p}-\sigma} + \hat{c}_{\mathbf{p}\sigma}^{\dagger} \hat{d}_{-\sigma}^{\dagger} \hat{d}_{-\sigma} \hat{c}_{\mathbf{k}\sigma} - \hat{c}_{\mathbf{p}-\sigma}^{\dagger} \hat{d}_{\sigma}^{\dagger} \hat{d}_{-\sigma} \hat{c}_{\mathbf{k}\sigma} \right) \\ & + \sum_{\mathbf{k}\mathbf{p}\sigma} \left[\frac{1}{\sqrt{N}} \eta_{\mathbf{k}}(l) V_{\mathbf{p}}(l) + \eta_{\mathbf{k}\mathbf{p}}(\xi_{\mathbf{p}}(l) - \xi_{\mathbf{k}}(l)) \right] \left(\hat{c}_{\mathbf{k}\sigma}^{\dagger} \hat{c}_{\mathbf{p}\sigma} + \hat{c}_{\mathbf{p}\sigma}^{\dagger} \hat{c}_{\mathbf{k}\sigma} \right) - \frac{2}{\sqrt{N}} \sum_{\mathbf{k}\sigma} \eta_{\mathbf{k}}(l) V_{\mathbf{k}}(l) \hat{d}_{\sigma}^{\dagger} \hat{d}_{\sigma} \\ & - \frac{2}{\sqrt{N}} \sum_{\mathbf{k}} \eta_{\mathbf{k}}^{(1)}(l) V_{\mathbf{k}}(l) \left(\hat{d}_{\uparrow}^{\dagger} \hat{d}_{\downarrow}^{\dagger} + \hat{d}_{\downarrow} \hat{d}_{\uparrow} \right) - \frac{2}{\sqrt{N}} \sum_{\mathbf{k}\sigma} \eta_{\mathbf{k}}^{(2)}(l) V_{\mathbf{k}}(l) \hat{d}_{\sigma}^{\dagger} \hat{d}_{-\sigma}^{\dagger} \hat{d}_{-\sigma} \hat{d}_{\sigma} \end{aligned}$$

$$\begin{aligned}
& + \sum_{\mathbf{k}\sigma} \left\{ \eta_{\mathbf{k}}(l) [\varepsilon_d(l) - \xi_{\mathbf{k}}(l)] + \frac{2}{\sqrt{N}} \sum_{\mathbf{p}} \eta_{\mathbf{k}\mathbf{p}}(l) V_{\mathbf{p}}(l) - \eta_{\mathbf{k}}^{(1)}(l) \Delta_d(l) \right\} \left(\hat{c}_{\mathbf{k}\sigma}^\dagger \hat{d}_\sigma + \hat{d}_\sigma^\dagger \hat{c}_{\mathbf{k}\sigma} \right) \\
& + \sum_{\mathbf{k}} \left\{ \eta_{\mathbf{k}}^{(1)}(l) U_d(l) - \eta_{\mathbf{k}}^{(2)}(l) \Delta_d(l) \right\} \left[\left(\hat{d}_\uparrow^\dagger \hat{d}_\uparrow \hat{d}_\downarrow^\dagger \hat{c}_{\mathbf{k}\uparrow}^\dagger - \hat{d}_\uparrow^\dagger \hat{c}_{\mathbf{k}\downarrow}^\dagger \hat{d}_\downarrow^\dagger \hat{d}_\downarrow \right) + \text{h.c.} \right] \\
& + \sum_{\mathbf{k}\sigma} \left\{ \eta_{\mathbf{k}}(l) U_d(l) + \eta_{\mathbf{k}}^{(2)}(l) [\varepsilon_d(l) - \xi_{\mathbf{k}}(l) + U_d(l)] \right\} \left(\hat{c}_{\mathbf{k}\sigma}^\dagger \hat{d}_\sigma \hat{d}_{-\sigma}^\dagger + \text{h.c.} \right) \\
& - \frac{1}{\sqrt{N}} \sum_{\mathbf{k}\mathbf{p}} \eta_{\mathbf{k}}^{(1)}(l) V_{\mathbf{p}}(l) \left[\left(\hat{c}_{\mathbf{k}\uparrow}^\dagger \hat{c}_{\mathbf{p}\downarrow}^\dagger + \hat{c}_{\mathbf{p}\uparrow}^\dagger \hat{c}_{\mathbf{k}\downarrow}^\dagger \right) + \text{h.c.} \right] - \frac{1}{\sqrt{N}} \sum_{\mathbf{k}\mathbf{p}\sigma} \eta_{\mathbf{k}}^{(2)}(l) V_{\mathbf{p}}(l) \left(\hat{c}_{\mathbf{k}\sigma}^\dagger \hat{c}_{\mathbf{p}-\sigma}^\dagger \hat{d}_{-\sigma} \hat{d}_\sigma + \text{h.c.} \right) \\
& - \sum_{\mathbf{k}} \left\{ \eta_{\mathbf{k}}(l) \Delta_d(l) + \eta_{\mathbf{k}}^{(1)}(l) [\xi_{\mathbf{k}}(l) + \varepsilon_d(l)] + \eta_{\mathbf{k}}^{(2)}(l) \Delta_d(l) \right\} \left[\left(\hat{c}_{\mathbf{k}\uparrow}^\dagger \hat{d}_\downarrow^\dagger + \hat{d}_\uparrow^\dagger \hat{c}_{\mathbf{k}\downarrow}^\dagger \right) + \text{h.c.} \right]. \quad (11)
\end{aligned}$$

On the right hand side of (11) we can notice several terms, which were initially absent in the model Hamiltonian (7). Some of them could be eliminated by a suitable modification of the generating operator $\hat{\eta}$ as it has been done for the usual Anderson model [4]. In the present study, however, we assume that the hybridization $V_{\mathbf{k}}$ is much smaller than all other parameters. This assumption allows us to simplify (11) using the linearizations

$$\begin{aligned}
[\hat{\eta}(l), \hat{H}(l)] & \approx \frac{1}{\sqrt{N}} \sum_{\mathbf{k}\mathbf{p}} \eta_{\mathbf{k}}^{(2)}(l) V_{\mathbf{p}}(l) \left(\hat{c}_{\mathbf{k}\uparrow}^\dagger \hat{d}_\downarrow^\dagger \hat{d}_\downarrow \hat{c}_{\mathbf{p}\uparrow}^\dagger - \hat{c}_{\mathbf{k}\downarrow}^\dagger \hat{d}_\uparrow^\dagger \hat{d}_\uparrow \hat{c}_{\mathbf{p}\downarrow}^\dagger + \hat{c}_{\mathbf{p}\uparrow}^\dagger \hat{d}_\downarrow^\dagger \hat{d}_\downarrow \hat{c}_{\mathbf{k}\uparrow}^\dagger - \hat{c}_{\mathbf{p}\downarrow}^\dagger \hat{d}_\uparrow^\dagger \hat{d}_\uparrow \hat{c}_{\mathbf{k}\downarrow}^\dagger \right) \\
& - \frac{2}{\sqrt{N}} \sum_{\mathbf{k}} \eta_{\mathbf{k}}^{(1)}(l) V_{\mathbf{k}}(l) \left(\hat{d}_\uparrow^\dagger \hat{d}_\downarrow^\dagger + \hat{d}_\downarrow \hat{d}_\uparrow \right) - \frac{2}{\sqrt{N}} \sum_{\mathbf{k}\sigma} \eta_{\mathbf{k}}^{(2)}(l) V_{\mathbf{k}}(l) \hat{d}_\sigma^\dagger \hat{d}_{-\sigma}^\dagger \hat{d}_{-\sigma} \hat{d}_\sigma \\
& + \sum_{\mathbf{k}\sigma} \left\{ \eta_{\mathbf{k}}(l) [\varepsilon_d(l) - \xi_{\mathbf{k}}(l) + U_d(l) \langle \hat{n}_{d,-\sigma} \rangle] + \frac{2}{\sqrt{N}} \sum_{\mathbf{p}} \eta_{\mathbf{k}\mathbf{p}}(l) V_{\mathbf{p}}(l) - \eta_{\mathbf{k}}^{(1)}(l) \Delta_d(l) \right. \\
& \left. + \eta_{\mathbf{k}}^{(2)}(l) [\varepsilon_d(l) - \xi_{\mathbf{k}}(l) + U_d(l)] \langle \hat{n}_{d,-\sigma} \rangle \right\} \left(\hat{c}_{\mathbf{k}\sigma}^\dagger \hat{d}_\sigma + \hat{d}_\sigma^\dagger \hat{c}_{\mathbf{k}\sigma} \right) + \hat{O}(l) \quad (12)
\end{aligned}$$

with the expectation value $\langle \hat{n}_{d,\sigma} \rangle = \langle \hat{d}_\sigma^\dagger \hat{d}_\sigma \rangle$ and the higher order term $\hat{O}(l)$ defined as

$$\begin{aligned}
\hat{O}(l) = & - \sum_{\mathbf{k}} \left\{ \eta_{\mathbf{k}}(l) \Delta_d(l) + \eta_{\mathbf{k}}^{(1)}(l) [\xi_{\mathbf{k}}(l) + \varepsilon_d(l) + U_d \langle \hat{n}_{d,\uparrow} \rangle] + \eta_{\mathbf{k}}^{(2)}(l) \Delta_d(l) (1 - \langle \hat{n}_{d,\uparrow} \rangle) \right\} \left(\hat{c}_{\mathbf{k}\uparrow}^\dagger \hat{d}_\downarrow^\dagger + \hat{d}_\downarrow \hat{c}_{\mathbf{k}\uparrow}^\dagger \right) \\
& - \sum_{\mathbf{k}} \left\{ \eta_{\mathbf{k}}(l) \Delta_d(l) + \eta_{\mathbf{k}}^{(1)}(l) [\xi_{\mathbf{k}}(l) + \varepsilon_d(l) + U_d \langle \hat{n}_{d,\downarrow} \rangle] + \eta_{\mathbf{k}}^{(2)}(l) \Delta_d(l) (1 - \langle \hat{n}_{d,\downarrow} \rangle) \right\} \left(\hat{d}_\uparrow^\dagger \hat{c}_{\mathbf{k}\downarrow}^\dagger + \hat{c}_{\mathbf{k}\downarrow} \hat{d}_\uparrow^\dagger \right) \\
& - \frac{1}{\sqrt{N}} \sum_{\mathbf{k}\mathbf{p}} \eta_{\mathbf{k}}^{(1)}(l) V_{\mathbf{p}}(l) \left[\left(\hat{c}_{\mathbf{k}\uparrow}^\dagger \hat{c}_{\mathbf{p}\downarrow}^\dagger + \hat{c}_{\mathbf{p}\uparrow}^\dagger \hat{c}_{\mathbf{k}\downarrow}^\dagger \right) + \text{h.c.} \right] - \frac{1}{\sqrt{N}} \sum_{\mathbf{k}\mathbf{p}\sigma} \eta_{\mathbf{k}}^{(2)}(l) V_{\mathbf{p}}(l) \left(\hat{c}_{\mathbf{k}\sigma}^\dagger \hat{c}_{\mathbf{p}-\sigma}^\dagger \hat{d}_{-\sigma} \hat{d}_\sigma + \text{h.c.} \right). \quad (13)
\end{aligned}$$

We next update the initial Hamiltonian (7) by the spin-exchange interaction $-\sum_{\mathbf{k},\mathbf{p}} J_{\mathbf{k}\mathbf{p}}(l) \hat{\mathbf{s}}_d \cdot \hat{\mathbf{S}}_{\mathbf{k}\mathbf{p}}$ imposing the initial condition $J_{\mathbf{k}\mathbf{p}}(0) = 0$. Neglecting the term (13) we finally obtain the set of coupled differential equations

$$\begin{aligned}
\frac{d\varepsilon_d(l)}{dl} &= -\frac{2}{\sqrt{N}} \sum_{\mathbf{k}} \eta_{\mathbf{k}}(l) V_{\mathbf{k}}(l) \\
\frac{dU_d(l)}{dl} &= -\frac{4}{\sqrt{N}} \sum_{\mathbf{k}} \eta_{\mathbf{k}}^{(2)}(l) V_{\mathbf{k}}(l) \\
\frac{d\Delta_d(l)}{dl} &= \frac{2}{\sqrt{N}} \sum_{\mathbf{k}} \eta_{\mathbf{k}}^{(1)}(l) V_{\mathbf{k}}(l) \\
\frac{dV_{\mathbf{k}}(l)}{dl} &= \eta_{\mathbf{k}}(l) [\varepsilon_d(l) - \xi_{\mathbf{k}}(l) + U_d(l) \langle \hat{n}_{d,-\sigma} \rangle]
\end{aligned}$$

$$\begin{aligned}
& - \eta_{\mathbf{k}}^{(1)}(l) \Delta_d(l) + \frac{2}{\sqrt{N}} \sum_{\mathbf{p}} \eta_{\mathbf{k}\mathbf{p}}(l) V_{\mathbf{p}}(l) \\
& + \eta_{\mathbf{k}}^{(2)}(l) [\varepsilon_d(l) - \xi_{\mathbf{k}}(l) + U_d(l)] \langle \hat{n}_{d,-\sigma} \rangle \\
\frac{dJ_{\mathbf{k}\mathbf{p}}(l)}{dl} &= \eta_{\mathbf{k}}^{(2)}(l) V_{\mathbf{p}}(l) + \eta_{\mathbf{p}}^{(2)}(l) V_{\mathbf{k}}(l) \\
& - (\xi_{\mathbf{k}} - \xi_{\mathbf{p}})^2 J_{\mathbf{k}\mathbf{p}}(l) \quad (14)
\end{aligned}$$

The spin exchange coupling $J_{\mathbf{k}\mathbf{p}}(l)$ appearing in the flow equation (14) can be treated within the lowest order analytical estimation. In the asymptotic limit $l \rightarrow \infty$ it evolves to

$$\begin{aligned}
J_{\mathbf{k}\mathbf{p}}(\infty) &= -2U_d V_{\mathbf{k}} V_{\mathbf{p}} \left\{ (\varepsilon_d - \xi_{\mathbf{k}})^2 + (\varepsilon_d - \xi_{\mathbf{p}})^2 \right. \\
& \left. + \Delta_d^2 - (\xi_{\mathbf{k}} + \xi_{\mathbf{p}}) U_d - (\xi_{\mathbf{k}} - \xi_{\mathbf{p}})^2 \right\}^{-1}. \quad (15)
\end{aligned}$$

and this fact is crucial for the Kondo effect.

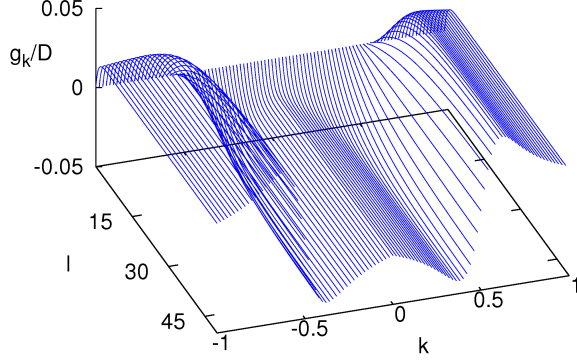


FIG. 3: The inter-species pairing potential $g_{\mathbf{k}}^{\sigma}(l)$ obtained numerically for the half-filled quantum dot using the same set of model parameters as in the main text.

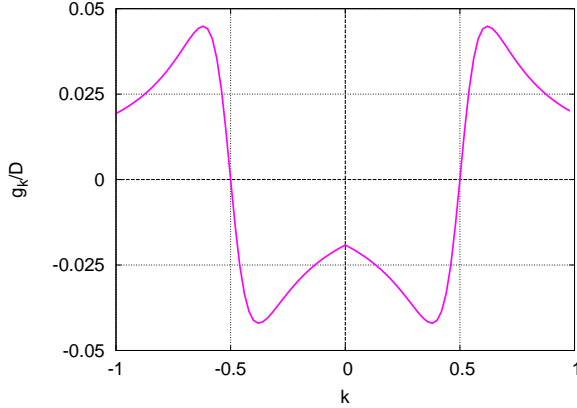


FIG. 4: The asymptotic value $g_{\mathbf{k}}^{\sigma}(\infty)$ of the potential displayed in figure 3.

For the half-filled quantum dot ($\varepsilon_d = -U_d/2$) its value near the Fermi surface becomes negative

$$J_{\mathbf{k}_F \mathbf{p}_F}(l \rightarrow \infty) = \frac{-4U_d|V_{\mathbf{k}_F}|^2}{U_d^2 + (2\Delta_d)^2} \quad (16)$$

C. Inter-species pairing

Besides the induced spin exchange interaction there can appear also other kinds of interactions. To give an example how such interactions can be studied in a systematic way we shall discuss here the exotic inter-species coupling specific for the proximized quantum dot (7). To take it into account we introduce the following l -dependent Hamiltonian

$$\begin{aligned} \hat{H}(l) = & \sum_{\mathbf{k}\sigma} \xi_{\mathbf{k}}(l) \hat{c}_{\mathbf{k}\sigma}^{\dagger} \hat{c}_{\mathbf{k}\sigma} + \sum_{\sigma} \varepsilon_d(l) \hat{d}_{\sigma}^{\dagger} \hat{d}_{\sigma} + U_d(l) \hat{n}_{d,\uparrow} \hat{n}_{d,\downarrow} \\ & - \left(\Delta_d(l) \hat{d}_{\uparrow}^{\dagger} \hat{d}_{\downarrow}^{\dagger} + \text{h.c.} \right) - \sum_{\mathbf{k}, \mathbf{p}} J_{\mathbf{k}\mathbf{p}}(l) \hat{\mathbf{s}}_d \cdot \hat{\mathbf{S}}_{\mathbf{k}\mathbf{p}} \\ & - \sum_{\mathbf{k}} \left[\left(g_{\mathbf{k}}^{\uparrow}(l) \hat{c}_{\mathbf{k}\uparrow}^{\dagger} \hat{d}_{\downarrow}^{\dagger} + g_{\mathbf{k}}^{\downarrow}(l) \hat{d}_{\uparrow}^{\dagger} \hat{c}_{\mathbf{k}\downarrow}^{\dagger} \right) + \text{h.c.} \right] \\ & + \sum_{\mathbf{k}\sigma} \left(V_{\mathbf{k}}(l) \hat{c}_{\mathbf{k}\sigma}^{\dagger} \hat{d}_{\sigma} + \text{h.c.} \right) \end{aligned} \quad (17)$$

with the initial condition $g^{\sigma}(0) = 0$. Repeating the same procedure as discussed in the previous section we obtain the additional flow equation for inter-species coupling

$$\frac{dg_{\mathbf{k}}^{\sigma}(l)}{dl} = [U_d(l) (2\langle \hat{n}_{d,\sigma} \rangle - 1) + 2\xi_{\mathbf{k}}] \Delta_d(l) V_{\mathbf{k}}(l). \quad (18)$$

For the half-filled quantum dot $\langle \hat{n}_{d,\sigma} \rangle = \frac{1}{2}$ this equation (18) simplifies to

$$\frac{dg_{\mathbf{k}}^{\sigma}(l)}{dl} = 2\xi_{\mathbf{k}} \Delta_d(l) V_{\mathbf{k}}(l). \quad (19)$$

Figure (3) shows the coupling $g_{\mathbf{k}}^{\sigma}(l)$ obtained numerically for the half-filled quantum dot. The next plot (4) illustrates the effective (asymptotic) value $g_{\mathbf{k}}^{\sigma}(\infty)$. We clearly notice that the inter-species pairing $g_{\mathbf{k}}^{\sigma}$ changes the sign around k_F . This property indicates the resonant character of such exotic interactions.

-
- [1] J. Bauer, A. Oguri, and A.C. Hewson, J. Phys.: Condens. Matter **19**, 486211 (2008).
 - [2] A.V. Balatsky, I. Vekhter, and J.-X. Zhu, Rev. Mod. Phys. **78**, 373 (2006).
 - [3] J. Barański and T. Domański, J. Phys.: Condens. Matter **25**, 435305 (2013).
 - [4] S. Kehrein and A. Mielke, Ann. Phys. **252**, 1-32 (1996);

- S. Kehrein and A. Mielke, J. Phys. A: Math. Gen. **27**, 4259-4279 (1994).
- [5] F. Wegner, Ann. Physik (Leipzig) **3**, 77 (1994).
- [6] S. Kehrein, *The flow equation approach to many-particle systems*, (Springer Tracts in Modern Physics **215**, Berlin, 2006).